A new long-term indentation relaxation method to measure creep properties at the micro-scale with application to fused silica and PMMA

P. Baral, G. Guillonneau, G. Kermouche, J.-M. Bergheau, J.-L. Loubet

Version of Record: https://www.sciencedirect.com/science/article/pii/S0167663619301255
Manuscript_a056f5b9ab87e0b71a096193fead8c78

A new long-term indentation relaxation method to measure creep properties at the micro-scale with application to fused silica and PMMA

P. Baral[a,b], G. Guillonneau[a], G. Kermouche[b], J.-M. Bergheau[c], J.-L. Loubet[a]

[a] *Univ. Lyon, Ecole Centrale de Lyon, CNRS UMR 5513 LTDS, F-69134, Ecully, France*
[b] *Mines Saint Etienne, Université de Lyon, CNRS UMR 5307 LGF, Centre SMS, F-42023, Saint Etienne, France*
[c] *Univ. Lyon, Ecole Nationale d'Ingénieurs de Saint Etienne, CNRS UMR 5513 LTDS, F-42023, Saint Etienne, France*

Abstract

A new procedure is developed to measure strain rate sensitivity m and apparent activation volume V^* using nanoindentation relaxation experiments. This procedure is based on the control of the dynamic contact stiffness as measured by the continuous stiffness measurement module (CSM). Load decrease is monitored while maintaining the contact stiffness constant. It allows for very stable measurements of load relaxation (up to 10 hours) since the contact area between the tip and the sample surface is kept constant. This improvement is significant as it increases by two orders of magnitude the measurement time compared to classical constant displacement experiments. The load relaxation data are interpreted using an analogy to uniaxial tests in order to extract representative material's parameters. An excellent agreement with literature data is found for fused silica and PMMA. Nanoindentation relaxation experiment is proved to be an accurate procedure to extract viscoplastic parameters of materials under very low strain rates.

Keywords:
Nanoindentation, relaxation, dynamic stiffness, fused silica, PMMA, creep, strain rate sensitivity, activation volume

1. Introduction

Probing the local time-dependent mechanical behavior of materials is getting more and more interest from the material community, especially concerning high temperature loadings. Deformation mechanisms are temperature and strain rate-dependent and are often defined from the study of strain rate sensitivity m and apparent activation volume V^*, which are closely related. A wide range of experimental methodologies have already been developed to extract such properties, going from creep and relaxation tests to constant strain rate (CSR) or strain rate jump (SRJ) tests (Wehrs et al. (2015)).

These methodologies can be applied to uniaxial loadings at nano-scale – i.e. micro-compression (Mohanty et al. (2016); Wehrs et al. (2017)) or traction (Guisbiers et al. (2013); Pardoen et al. (2016)) – as it is performed on the bulk. Still, these techniques require careful preparation steps. Nanoindentation, even generating a complex stress and strain gradient beneath the tip, remains a reliable mechanical characterization set-up.

The common limitation to all these tests procedures is the system stability. More precisely, thermal drift can cause large errors in displacement measurements. Even at room temperature, tests longer than five to ten minutes are subject to inaccuracies. In the case of nanoindentation, two ways have been followed to overcome this issue. The first one is to limit the indentation time, and hence focus on relatively fast deformation kinetics as during CSR or SRJ tests (Maier et al. (2011)). The second is based on the dynamic measurement of the contact stiffness (Oliver and Pharr (1992)) which is almost insensitive to thermal drift and allows for long-term mechanical characterizations.

This latter has been first applied by Syed Asif and Pethica (1997) to monitor the increase in contact area as a function of time while maintaining the load constant (CLH tests). Goldsby et al. (2004) performed such tests up to 13 hours hold period at room temperature and Maier et al. (2013) applied it to high temperature characterization of ultra fine grain aluminum up to 10 hours duration.

However, nanoindentation creep tests are prone to interpretation issues depending on the material behavior and homogeneity. Indeed, during the hold load segment, the indentation-affected volume increases continuously. Therefore, in the case of thin film characterization, where the hardness and Young modulus strongly depend on the indentation depth, the CLH test

would be a measurement of both viscoplastic and depth-dependent mechanical behavior. Besides, as the indentation affected volume increases, more and more material enters primary creep. For this latter reason, Goodall and Clyne (2006) claimed that the use of CLH tests could lead to discrepancies in determining the fundamental creep characteristics. Yet, these uncertainties can be minimized for materials exhibiting a small primary creep region compared to stationary creep (Baral et al. (2017); Phani and Oliver (2016)).

Nanoindentation relaxation tests might appear to be better candidates to obtain the material's creep parameters in a wider range of conditions, since the affected volume is not supposed to vary significantly during the hold segment.

To the authors best knowledge, all the indentation relaxation tests were performed at constant displacement (Sakai et al. (2005); Mattice et al. (2006); Zhang et al. (2006); Stegall et al. (2014); Baral et al. (2017)). This loading procedure is relatively easy to implement but is subjected to thermal drift issues. Hence, relaxation measurements were limited to several minutes at best, as stated before.

The present work aims to develop a new indentation relaxation method to measure creep properties at very low strain rates – i.e. over a long period of time – without applying thermal drift corrections. First, the procedure based on the control of the dynamic contact stiffness to maintain a constant contact area is detailed. Then an analytical development is proposed to transform raw data into stress and strain rate, to measure strain rate sensitivities m and apparent activation volumes V^*. Applications of this new long-term indentation relaxation test to fused silica and PMMA are performed. Finally indentation results are compared to creep literature data, both at the micro and macro-scale.

2. Theoretical framework

2.1. Stiffness measurements and contact area

The continuous stiffness measurement (CSM) module developed by Oliver and Pharr (1992) allows to measure contact stiffness as a function of time. It has been assessed by several authors (Oliver and Pharr (1992); Syed Asif and Pethica (1997)) that contact area is proportional to the contact stiffness as long as the materials' modulus is not indentation depth-dependent. Hence, the following relation is used (Oliver and Pharr (1992)):

$$S(\omega) = 2E_c'^*(\omega)\sqrt{\frac{A_c}{\pi}} \tag{1}$$

Where $E_c'^*(\omega)$ is the reduced contact modulus (Loubet et al. (1993)) measured at a given frequency ω and A_c is the contact area. The contact depth h_c is calculated from the Oliver and Pharr method (Oliver and Pharr (1992)). Calculations are detailed in reference (Baral et al. (2017)). The contact area A_c is then calculated from a cone of equivalent inclined face angle β:

$$A_c = \pi.\left(\frac{h_c}{\tan(\beta)}\right)^2 \tag{2}$$

For an equivalent Berkovich indenter, $\beta = 19.68°$.

2.2. Derivation of stress relaxation

The calculation of a representative stress under conical and, by extension, pyramidal tips is primordial to compare quantitatively uniaxial and nanoindentation tests. To perform such a comparison, Kermouche et al. (2008) propose a definition of representative stress based on the conical indentation of an elastoplastic solid. Equation 3 gives the representative stress as a function of the measured hardness H and Young modulus E'. The relation also depends on the equivalent cone inclined face angle β and on geometrical constants ζ_1, ζ_2 and ζ_3.

For a Berkovich tip $\zeta_1 = 0.66$, $\zeta_2 = 0.216$ and $\zeta_3 = 0.24$ (Kermouche et al. (2008)).

$$\sigma_r = \frac{\zeta_3 \tan(\beta) H}{\zeta_1 \tan(\beta) - (1-\zeta_2)\frac{H}{E'}} \tag{3}$$

In order to calculate the strain rate sensitivity m and apparent activation volume V^*, the representative strain rate beneath the tip must be known. Here again, an analogy to uniaxial tests is proposed.

In the framework of uniaxial relaxation, the strain is kept constant over a certain period of time while the material's stress relaxation is monitored. In this study, we consider a Bingham-Norton elasto-viscoplastic model expressed such as $\sigma = E\epsilon$ in the elastic regime and $\sigma = \sigma_y + K(\dot{\epsilon}_{vp})^m$ in the viscoplastic regime, with E the Young modulus, σ_y the yield stress, m the strain rate sensitivity and K the consistency (see figure 1b). According to this model,

we can write the total uniaxial strain and stress such as $\epsilon = \epsilon_e + \epsilon_{vp} = cst$ and $\sigma = \sigma_e = \sigma_{vp}$. With ϵ_e and ϵ_{vp} the elastic and viscoplastic components of the total strain and their corresponding stresses σ_e and σ_{vp}.

Based on these equations, it follows, by taking the derivative of the strain with respect to time, that $\dot{\epsilon}_{vp} = \ -\dot{\epsilon}_e$. Also, the stress is related to the elastic strain through $\sigma = E'\epsilon_e$. The derivative of this relation with respect to time then leads to $|\dot{\epsilon}_{vp}| = \frac{|\dot{\sigma}|}{E'}$.This expresses the viscoplastic strain rate as a function only of the elastic properties and the applied stress.

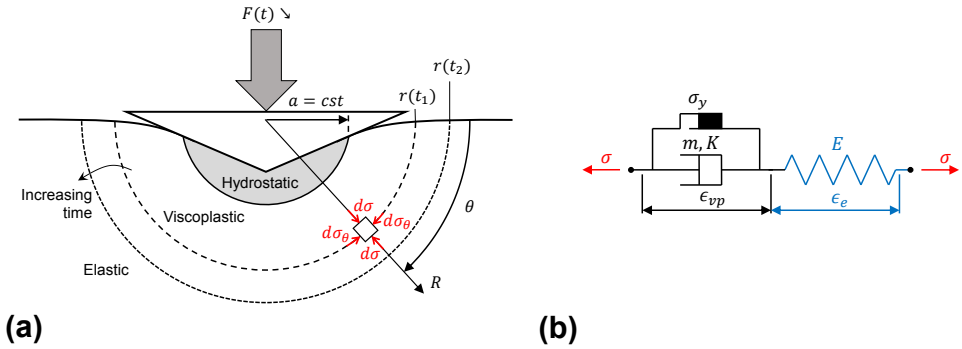

Figure 1: (a) Schema of the expending hemispherical viscoplastic core under conical indentation, adapted from Johnson (1970). (b) Corresponding uniaxial Bingham-Norton elasto-viscoplastic model characterized by the yield stress σ_y, the strain rate sensitivity m and the consistency K.

From this formulation, an equivalent viscoplastic indentation strain rate could be determined. This has been done by Xu et al. (2010) in the framework of flat punch indentation. Here, we propose to extrapolate the classical uniaxial formulation for conical (or pyramidal) indentation.

Figure 1a is a schematic representation of deformation states under a conical (or pyramidal) tip. This schema is based on the model of Hill, which has been taken over by Johnson (1970). It represents the expending hemispherical viscoplastic core of radius $r(t)$ under conical indentation. At constant contact area – i.e. constant indented volume – the hemispherical viscoplastic core increases until equilibrium is reached between the overall elastic stress beneath the core and the stress in the core. This expansion is represented by the two hemispheres of radius $r(t)$ at time t_1 and t_2 such as $t_2 > t_1$.

In analogy with the uniaxial case, the viscoplastic strain rate is expressed by the following equation:

$$|\dot{\epsilon}_{vp}| = \frac{|\dot{\sigma}_r|}{E'} \tag{4}$$

With E' the Young modulus of the material and σ_r the representative stress calculated from expression 3.

2.3. Strain rate sensitivity

In uniaxial tests the strain rate sensitivity m characterizes the variation of yield stress with the corresponding applied strain rate. In indentation this mechanical property is defined as the variation of hardness with applied strain rate as expressed by the following equation:

$$m_i = \frac{d \ln H}{d \ln \dot{\epsilon}_{vp}} \tag{5}$$

It must be noted that the strain rate used in the usual formulation is defined by $\dot{\epsilon} = \dot{h}/h$, however in the case of indentation relaxation tests: $\dot{h} = 0$, so equation 4 must be used instead.

In the framework of rigid viscoplastic solids, equation 5 corresponds exactly to the uniaxial formulation. However, several authors have shown that this equivalence is not valid in the case of elasto-viscoplastic solids (Kermouche et al. (2006); Elmustafa et al. (2007); Stone et al. (2010)) because the ratio between representative stress over hardness (σ_r/H) evolves with the ratio (H/E').

Hence, Kermouche et al. (2006) propose to use the representative stress defined by equation 3 to derive the effective strain rate sensitivity m of the material:

$$m = \frac{d \ln \sigma_r}{d \ln \dot{\epsilon}_{vp}} \tag{6}$$

In the following developments, both of the strain rate sensitivities formulations will be compared to literature references.

2.4. Apparent activation volume

The apparent activation volume V^* is characteristic of the rate deformation process and is somehow related to the number of atoms or molecule

segments involved in the material's plastic deformation. It is proportional to the inverse of the strain rate sensitivity m. Equation 7 is directly derived from the uniaxial definition of the apparent activation volume, with k the Boltzmann constant and T the absolute temperature (Chen et al. (2005); Gu et al. (2007)). The stress and strain rate are replaced by representative nanoindentation stress σ_r and strain rate $\dot{\epsilon}_{vp}$.

$$V^* = \sqrt{3}kT\Big(\frac{d\ln\dot{\epsilon}_{vp}}{d\sigma_r}\Big) \tag{7}$$

3. Materials and methods

The materials studied in this work were fused silica (FS) and Poly(methyl methacrylate) (PMMA). Fused silica was used as a reference material to state on the validity of nanoindentation measurements. PMMA sample was a commercial polymer in the form of 4 mm thick slab. Each sample had optical finishing with an arithmetic average roughness around 1 nm.

Nanoindentation relaxation experiments were performed with a nanoindenter SA2® (Keysight Technologies, Santa Rosa, California) with a Dynamic Contact Module (DCM) head that allows for very accurate measurements at low load and displacement. The indentation set-up is load-controlled with a maximum force of 10 mN and a resolution of 1 nN. Displacement is measured with a resolution of 0.2 pm.

Constant strain rate (CSR) experiments have been performed on PMMA for comparison with the new procedure developed. Six strain rates have been used ($\dot{h}/h = 2.5\times10^{-3}$; 5×10^{-3} ; 1×10^{-2} ; 2.5×10^{-2} ; 5×10^{-2} ; 1.5×10^{-1} s^{-1}). Loading were carried out up to a maximum depth of 500 nm. The continuous stiffness measurement (CSM) was set up at a frequency of 75 Hz with an amplitude of 1 nm. For each loading conditions five experiments were performed.

For long-term relaxation tests the following procedure has been carried out:

The continuous stiffness measurement (CSM) was set up at a frequency of 43 Hz for PMMA and 75 Hz for FS. The oscillation amplitude was set to 8 nm for PMMA and to 3 nm for FS. Loading parameters are displayed in table 1, where $\dot{h}/h$ is the strain rate measured while applying a constant $\dot{P}/P$ during loading, S_1 is the contact stiffness during the hold segment and h_{equiv}, the equivalent displacement into the sample.

Table 1: Loading parameters for the constant contact stiffness relaxation procedure.

Mater.	Hold duration (h)	$\dot{h}/h$ (s^{-1})	S_1 ($N.m^{-1}$)	h_{equiv} (nm)
Fused silica	5	0.05	5×10^4	200
PMMA	10	0.05	1.44×10^4	500

The contact stiffness was controlled with a PID loop where only proportional and integral gain were tuned. A particular care was taken to minimize the time response to reach the target value and the overshoot of the system. For PMMA, the best set of gains found allows for a time response of around 10 s with an overshoot of 3.8 % and a contact stiffness maintained within ±45 $N.m^{-1}$. For fused silica, no overshoot nor critical time response could be characterize above the noise level (±500 $N.m^{-1}$).

The hardness H is calculated, during the relaxation segment, by the following relation:

$$H = \frac{F}{A_c} = \frac{4F}{\pi}\Big(\frac{E_c'^*(\omega)}{S(\omega)}\Big)^2 \tag{8}$$

It is assumed that $E_c'^*(\omega)$ is independent of time at constant applied frequency ω. The value of the reduced contact modulus is calculated from the end of the loading segment, with the CSM module. The stiffness $S(\omega)$ is kept constant and the force decreases. Hence, equation 3 can be calculated based on expression 8.

To calculate the viscoplastic strain rate, the representative stress is post-treated to decrease the noise to signal ratio prior numerical differentiation. This treatment consists of a re-sampling of the force signal at a constant spacing of 0.02 on log-time scale. The set of data is then averaged (based on 3 relaxation curves for FS and 5 for PMMA). At the end, a moving average on 50 points is realized. This final post-treatment reduces greatly the numerical noise generated by the derivative without modifying the general trend of the representative stress.

The loading kinetics prior the relaxation segment does not affect the measured strain rate sensitivity, it just defines the range of strain rates available

during the relaxation segment. Hence, the maximum strain rate measurable in relaxation depends on the strain rate during loading – i.e. higher is the loading strain rate, higher will be the maximum strain rate during relaxation.

Concerning the characterization of m and V^*, there is no cut-off time to account for, contrary to characterization of *time*-dependent behavior such as relaxation modulus (Baral et al. (2017)).

Furthermore, the application of a high strain rate during loading causes control issues at the beginning of the relaxation segment. Thus, it is not necessary to perform such loading since potentially high strain rate relaxation data will be altered by the overshoot issues.

4. Results

4.1. Constant displacement vs. constant stiffness

Figure 2 displays classical relaxation tests performed by imposing a constant displacement. Load, contact stiffness and penetration depth are represented as a function of time for 1 hour constant displacement tests on PMMA. Both load and stiffness signals diverge after 10 minutes which clearly indicates a thermal drift issue.

Figure 3 displays the application of the constant contact stiffness relaxation test on PMMA, during 2 hours. Four tests were performed with an excellent repeatability, regarding the force signal, over the whole tested period. Displacement, however shows some large drift and no-repeatability. This feature is very interesting for several reasons:

- First, a direct measure of thermal drift, independent of the material's mechanical behavior – i.e. creep – is made possible.
- Secondly, for most cases, the assumption of a constant drift rate seems to hold true even during long periods of test.

It is proved experimentally that maintaining the contact stiffness constant is equivalent to keeping the contact area constant. Thus, creep parameters can be characterized accurately on a larger time-scale with constant contact stiffness (10^4 s) rather than constant displacement (10^2 s).

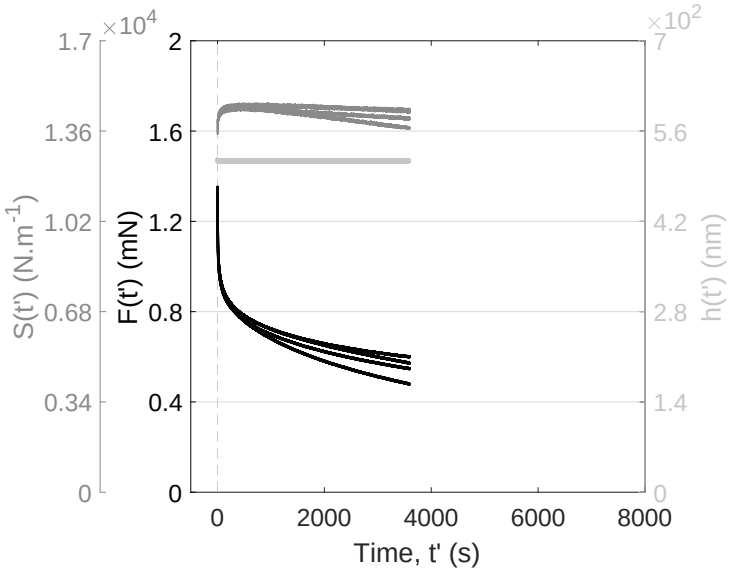

Figure 2: Indentation relaxation tests performed at constant displacement during 1 hour on PMMA. Displacement, force and stiffness evolution while maintaining a constant penetration depth are displayed versus relaxation time, t'. $t' = 0$ corresponds to the transition between the loading segment and constant displacement.

4.2. Strain rate dependent behavior of fused silica

Figure 4 displays the evolution of strain rate with hardness for fused silica at room temperature. Long-term relaxation result is compared to nanoindentation creep data from Elmustafa and Stone (2007). An excellent agreement is found between the two sets of data.

The strain rate sensitivity m_i calculated from the variation of hardness (equation 5) based on the relaxation measurements is equal to 0.016. Elmustafa and Stone (2007) found very similar result with nanoindentation creep tests ($m_i = 0.015 \pm 0.002$).

The long-term relaxation test developed here permits to state that the power law relation between stress and strain rate for fused silica holds true even at very low strain rates (between $\dot{\epsilon}_{vp} = 10^{-4}$ s^{-1} and 10^{-7} s^{-1}).

It is also interesting to note that the strain rate sensitivity as determined by the representative stress σ_r (m from equation 6) is significantly different from the variation of hardness. Indeed, m_i is necessarily lower than m since σ_r depends on the ratio H/E' which change continuously during relaxation

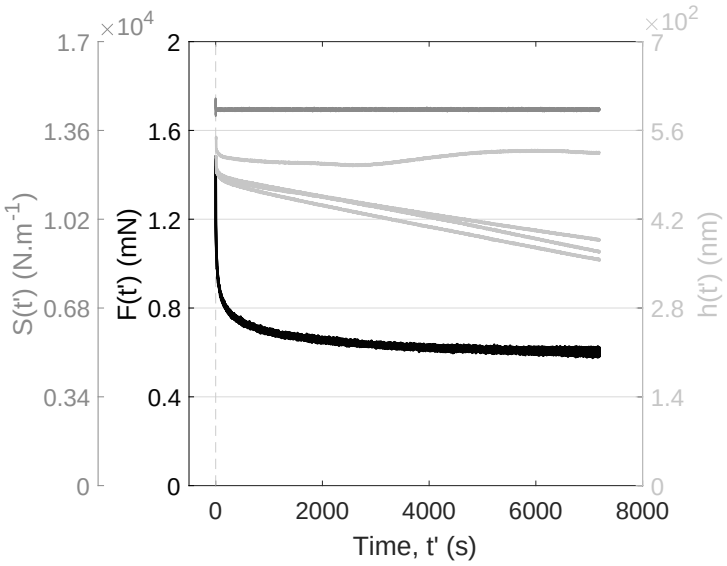

Figure 3: Indentation relaxation test performed at constant stiffness over 2 hours on PMMA. Displacement, force and stiffness evolution while maintaining a constant contact stiffness are displayed versus relaxation time, t'. $t' = 0$ corresponds to the transition between the loading segment and constant stiffness.

(or creep) (Kermouche et al. (2006, 2007); Elmustafa and Stone (2007)). From numerical simulation Elmustafa and Stone (2007) determined the relation between the ratio m_i/m as a function of H/E'. Hence, they found a strain rate sensitivity $m = 0.022$ which is consistent with our result from equation 6, $m = 0.029$.

In order to compare the apparent activation volume obtained in our case with the one coming from the work of Elmustafa and Stone (2007), the same definition of V^* must be adopted. As Elmustafa and Stone used $V^* = 3kT/m\sigma$ instead of $V^* = \sqrt{3}kT/m\sigma$, dividing their result ($V^* = 0.13\ nm^3$) by $\sqrt{3}$ leads to $V^* = 0.075\ nm^3$ which is closer to our result $V^* = 0.047\ nm^3$.

These good agreements allow us to validate the theoretical approach developed in section 2.2 for the calculation of the viscoplastic strain rate during relaxation. It also proves the ability to perform quantitative measurements of strain rate sensitivity under very low strain rates – i.e. comparable to classical long-term uniaxial relaxation experiments.

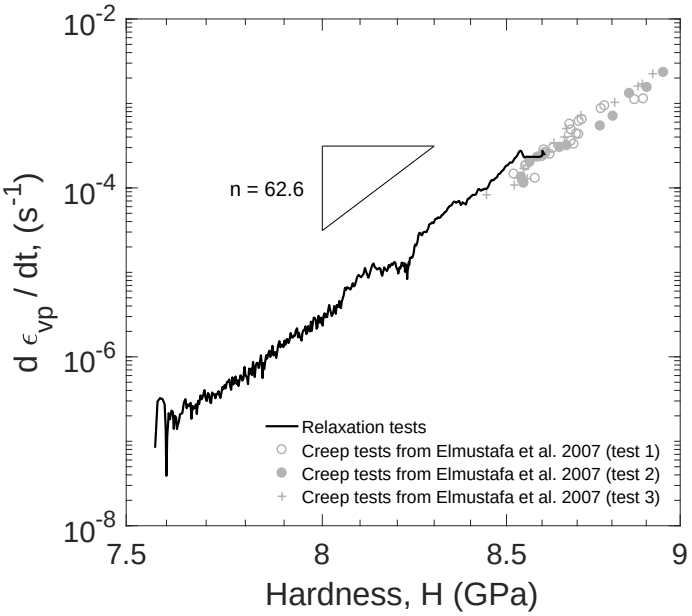

Figure 4: Strain rate *vs.* hardness for fused silica

4.3. Strain rate dependent behavior of PMMA

Figure 5 displays the evolution of strain rate with representative stress for PMMA. Long-term relaxation test is compared to constant strain rate (CSR) nanoindentation tests and literature data from uniaxial macroscopic compression realized by Richeton et al. (2006).

It must be pointed out that values of representative stress σ_r and compressive yield stress σ_y are not obtained at the same strain level. Indeed, with a Berkovich tip the plastic strain applied to the material is about 10 % (Kermouche et al. (2008)) (compared to $\epsilon_p(\sigma_y) \approx 0$ % for uniaxial compression). It is well known that a softening effect appears in uniaxial compression of PMMA for $\epsilon > \epsilon_y$, with ϵ_y the total strain at yield point (Richeton et al. (2006)), hence, $\sigma_r < \sigma_y$. However, at very low strain rates, typically $\dot{\epsilon} < 0.01$ s^{-1}, there is almost no softening, as can be seen on the stress-strain curves from Richeton et al. (2006). Accordingly, one can state that $\sigma_r \approx \sigma_y$.

Considering this approximation, all the results follow the same trend, characterized by two segments :

- For intermediate strain rates ($10^{-4} < \dot{\epsilon}_{vp} < 10$ s^{-1}) $\dot{\epsilon}_{vp}$ varies linearly with the representative stress (or yield stress) in a loglog scale ;

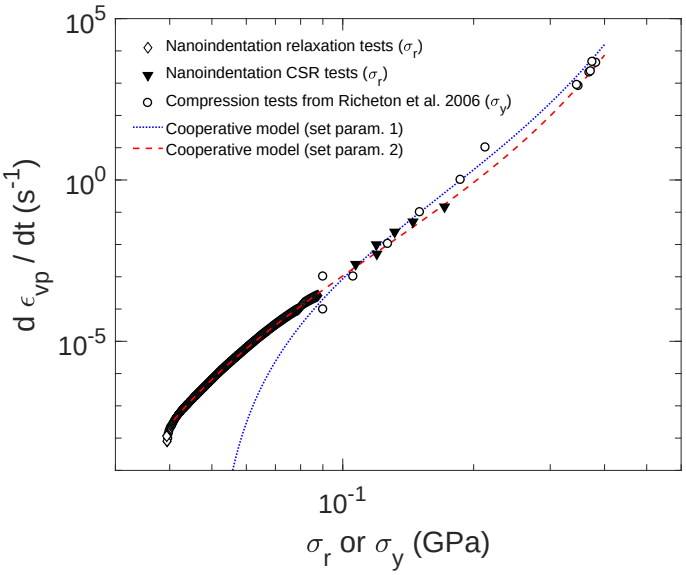

Figure 5: Strain rate *vs.* representative stress during 10 h constant contact stiffness experiment for PMMA, compared to nanoindentation CSR tests and macro-scale compression tests performed by Richeton et al. (2006). The blue and red dashed lines represent the cooperative model from Richeton et al. (2006) for two sets of parameters defined in table 2.

- and for low strain rates ($10^{-8} < \dot{\epsilon}_{vp} < 10^{-4}$ s^{-1}) the power law relation does not hold true.

This description is consistent with the cooperative model proposed by Richeton et al. (2006) which is composed of six parameters such as $\dot{\epsilon}_0$ the pre-exponential strain rate, ΔH_β the β relaxation activation energy, V the activation volume, $\sigma_i(0)$ the internal stress at zero Kelvin, m_C a material constant and n a material parameter used to depict the cooperative movement of the chain segments. The trend of this model is shown on figure 5 for two sets of parameters (displayed in table 2). The first set (blue dashed line) has been fitted on the strain rate range [$10^{-4} < \dot{\epsilon}_{vp} < 10^{4}$ s^{-1}] (Richeton et al. (2007)) which is not representative of our long-term relaxation test. Hence, it fails to predict the strain rate sensitivity of PMMA in the range [$10^{-8} < \dot{\epsilon}_{vp} < 10^{-4}$ s^{-1}].

Nevertheless, one could find a physically-correct set of parameters to model yield stress of PMMA on the entire range of strain rates [$10^{-8} <$

$\dot{\epsilon}_{vp} < 10^4$ s^{-1}]. This is shown in figure 5 with the set of parameters 2, given in table 2, which we propose.

Table 2: Cooperative model parameters proposed by Richeton et al. (2007) (set 1) and adjusted to our relaxation results (set 2).

Param.	Set 1	Set 2
$\dot{\epsilon}_0$ (s^{-1})	7.46×10^{15}	4.00×10^{16}
ΔH_β (kJ/mol)	90	100
V (m^3)	5.14×10^{-29}	5.14×10^{-29}
$\sigma_i(0)$ (MPa)	190	170
m_C (MPa/K)	0.47	0.49
n	6.37	6.70

It is not stated here that the set of parameters 2 is more representative than the one from Richeton et al. (2007). It just confirms that long-term relaxation data are deeply related to the underlying physical process, since the set of parameters 2 is just a little variation of the one proposed by Richeton et al. (2007).

Figure 6a displays the strain rate sensitivity m as calculated by equation 6 for the long-term relaxation test and the CSR tests performed on PMMA. For the calculus of m from relaxation experiments, a linear fit is performed on 51 points and the strain rate associated with the fit result is taken at the middle of the studied segment.

Here again, the results obtained from relaxation tests are in very good agreement with the CSR ones. Strain rate sensitivity of PMMA is characterized around $m = 0.1$ until $\dot{\epsilon}_{vp} = 10^{-4}$ s^{-1} (Kermouche et al. (2006)), then it decreases with decreasing strain rate, as expected from figure 5.

Figure 6b displays the evolution of apparent activation volume V^* as a function of strain rate. V^* increases as the strain rate decreases under $\dot{\epsilon}_{vp} = 10^{-4}$ s^{-1}.

According to the cooperative model proposed by Richeton et al. (2007), the apparent activation volume V^* significantly increases at low strain rates. Even if the physical meaning of the activation volume is not perfectly defined,

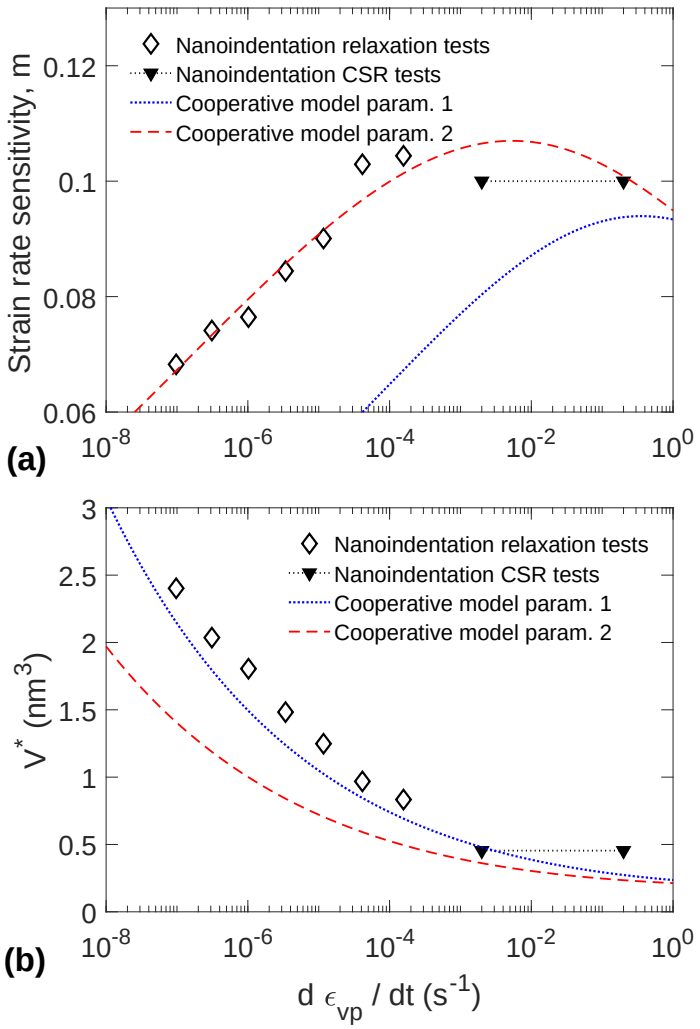

Figure 6: Strain rate sensitivity *vs.* strain rate during 10 h constant contact stiffness experiment for PMMA compared to nanoindentation CSR tests. The blue and red dashed lines represent the cooperative model from Richeton et al. (2006) for the two sets of parameters defined in table 2.

in the case of glassy polymers, the relaxation process is often related to intramolecular and intermolecular motions. Thus, the activation volume would indicate the number of chain segments involved in the plastic deformation process (Varnik et al. (2004); Richeton et al. (2007)).

At low strain rates intermolecular motions are enhanced by the reduction of the interactions between chains (Richeton et al. (2007)). Varnik et al. (2004) report, based on molecular dynamics simulation, a change in the slope of $\log(\dot{\epsilon})$ *vs.* σ_y at low strain rates. From this observation they determine a cross over strain rate. This feature is observed in our relaxation experiments and the cross over strain rate could be determined between $10^{-4} < \dot{\epsilon}_{vp} < 10^{-3}$ s^{-1}. At lower strain rates, they suggest that the change in slope is related to an enhancement of the stress release due to inherent structural relaxation (Varnik et al. (2004)).

It is also necessary to note that, in the case of polymers, the stress relaxation process can be both viscoelastic and viscoplastic. Thus, the material Young's modulus may decrease as relaxation happened.

According to equation 4, a decrease of the modulus leads to an increase of the strain rate $\dot{\epsilon}_{vp}$, which means that our calculations tend to underestimate the strain rate for long relaxation duration. Nevertheless, in the case of PMMA, considering a relaxed modulus of $E' = 2.5\ GPa$ after 10 hours at room temperature (Fernández et al. (2011)) does not introduce a significant modification of the calculated strain rate sensitivity m and apparent activation volume V^*.

5. Conclusions

A long-term nanoindentation relaxation test has been developed based on the control of contact stiffness during the experiment and several highlights can be extracted from this work:

- By keeping the contact stiffness constant over time, a constant contact area can be established between the tip and the material. This increases the measurement time-scale by two orders of magnitude compared to classical constant displacement procedures – i.e. from 10^2 s to 10^4 s hold period.

- Constant stiffness relaxation and indentation creep tests give similar results when testing homogeneous materials. Yet, the constant indented

volume implied by the relaxation method is a great asset concerning characterization of thin films.

- Measurements of stress relaxation have been performed on fused silica and PMMA samples. Strain rate sensitivities m and apparent activation volumes V^* were obtained at strain rates down to 10^{-8} s^{-1} thanks to the newly developed long-term relaxation tests and compared to literature values.

- For fused silica, an excellent agreement was found between nanoindentation constant load creep tests and our results. The new input of the long-term relaxation method permits to state that fused silica behave as a power law viscoplastic solid on a wide range of strain rate $[10^{-7} < \dot{\epsilon} < 10^{-2}$ $s^{-1}]$.

- For PMMA, a decent agreement is found between CSR nanoindentation tests, macroscopic uniaxial compression tests (Richeton et al. (2006)) and relaxation data. Here again, all curves follow the same trend on a wide range of strain rates $[10^{-8} < \dot{\epsilon} < 10^{4}$ $s^{-1}]$. As expected from molecular dynamics simulation (Varnik et al. (2004)), the slope of $\log(\dot{\epsilon})$ *vs.* σ changes at low strain rates.

- For PMMA, an increase in the apparent activation volume V^* associated with a decrease of the strain rate sensitivity m when decreasing the strain rate, referred in the literature (Varnik et al. (2004); Richeton et al. (2007)), is highlighted by means of the long-term relaxation experiment.

A clear prospective to this work is to perform relaxation experiments on thin films and at higher temperatures to explore with more insight the activation parameters of slow rate deformation processes in metals.

Acknowledgments

This work was supported by the LABEX MANUTECH-SISE (ANR-10-LABX-0075) of Université de Lyon within the program "Investissements d'Avenir" (ANR-11-IDEX-0007) operated by the French National Agency (ANR). The authors would also like to acknowledge financial support from Institut Carnot Ingénierie@Lyon.

References

Baral, P., Guillonneau, G., Kermouche, G., Bergheau, J. M., Loubet, J. L., 2017. Theoretical and experimental analysis of indentation relaxation test. Journal of Materials Research.

Chen, J., Shi, Y., Lu, K., nov 2005. Strain Rate Sensitivity of a Nanocrystalline CuNiP Alloy. Journal of Materials Research 20 (11), 2955–2959.

Elmustafa, A., Kose, S., Stone, D., apr 2007. The strain-rate sensitivity of the hardness in indentation creep. Journal of Materials Research 22 (04), 926–936.

Elmustafa, A., Stone, D., oct 2007. Strain rate sensitivity in nanoindentation creep of hard materials. Journal of Materials Research 22 (10), 2912–2916.

Fernández, P., Rodríguez, D., Lamela, M. J., Fernández-Canteli, A., 2011. Study of the interconversion between viscoelastic behaviour functions of PMMA. Mechanics of Time-Dependent Materials 15 (2), 169–180.

Goldsby, D. L., Rar, A., Pharr, G. M., Tullis, T. E., jan 2004. Nanoindentation creep of quartz, with implications for rate- and state-variable friction laws relevant to earthquake mechanics. Journal of Materials Research 19 (01), 357–365.

Goodall, R., Clyne, T. W., 2006. A critical appraisal of the extraction of creep parameters from nanoindentation data obtained at room temperature. Acta Materialia 54 (20), 5489–5499.

Gu, C. D., Lian, J. S., Jiang, Q., Zheng, W. T., dec 2007. Experimental and modelling investigations on strain rate sensitivity of an electrodeposited 20 nm grain sized Ni. Journal of Physics D: Applied Physics 40 (23), 7440–7446.

Guisbiers, G., Colla, M.-S., Coulombier, M., Raskin, J.-P., Pardoen, T., jan 2013. Study of creep/relaxation mechanisms in thin freestanding nanocrystalline palladium films through the lab-on-chip technology. Journal of Applied Physics 113 (2), 024513.

Johnson, K. L., apr 1970. The correlation of indentation experiments. Journal of the Mechanics and Physics of Solids 18 (2), 115–126.

Kermouche, G., Loubet, J. L., Bergheau, J. M., 2006. A new index to estimate the strain rate sensitivity of glassy polymers using conical/pyramidal indentation. Philosophical Magazine 86 (33-35), 5667–5677.

Kermouche, G., Loubet, J. L., Bergheau, J. M., 2007. Cone indentation of time-dependent materials: The effects of the indentation strain rate. Mechanics of Materials 39 (1), 24–38.

Kermouche, G., Loubet, J. L., Bergheau, J. M., 2008. Extraction of stress-strain curves of elastic-viscoplastic solids using conical/pyramidal indentation testing with application to polymers. Mechanics of Materials 40 (4-5), 271–283.

Loubet, J. L., Bauer, M., Tonck, A., Bec, S., Gauthier-Manuel, B., 1993. Nanoindentation with a Surface Force Apparatus. In: Mechanical Properties and Deformation Behavior of Materials Having Ultra-Fine Microstructures. Vol. 233. Springer Netherlands, Dordrecht, pp. 429–447.

Maier, V., Durst, K., Mueller, J., Backes, B., Höppel, H. W., Göken, M., 2011. Nanoindentation strain-rate jump tests for determining the local strain-rate sensitivity in nanocrystalline Ni and ultrafine-grained Al. Journal of Materials Research 26 (11), 1421–1430.

Maier, V., Merle, B., Göken, M., Durst, K., 2013. An improved long-term nanoindentation creep testing approach for studying the local deformation processes in nanocrystalline metals at room and elevated temperatures. Journal of Materials Research 28 (09), 1177–1188.

Mattice, J., Lau, A., Oyen, M., Went, R., 2006. Spherical indentation load-relaxation of soft biological tissues. Journal of Materials Research 21, 2003–2010.

Mohanty, G., Wehrs, J., Boyce, B. L., Taylor, A., Hasegawa, M., Philippe, L., Michler, J., 2016. Room temperature stress relaxation in nanocrystalline Ni measured by micropillar compression and miniature tension. Journal of Materials Research, 1–11.

Oliver, W. C., Pharr, G. M., 1992. An improved technique for determining hardness and elastic modulus using load and displacement sensing indentation experiments.

Pardoen, T., Colla, M.-S., Idrissi, H., Amin-Ahmadi, B., Wang, B., Schryvers, D., Bhaskar, U. K., Raskin, J.-P., mar 2016. A versatile lab-on-chip test platform to characterize elementary deformation mechanisms and electromechanical couplings in nanoscopic objects. Comptes Rendus Physique 17 (3-4), 485–495.

Phani, P. S., Oliver, W. C., 2016. A direct comparison of high temperature nanoindentation creep and uniaxial creep measurements for commercial purity aluminum. Acta Materialia 111, 31–38.

Richeton, J., Ahzi, S., Daridon, L., aug 2007. Thermodynamic investigation of yield-stress models for amorphous polymers. Philosophical Magazine 87 (24), 3629–3643.

Richeton, J., Ahzi, S., Vecchio, K. S., Jiang, F. C., Adharapurapu, R. R., 2006. Influence of temperature and strain rate on the mechanical behavior of three amorphous polymers: Characterization and modeling of the compressive yield stress. International Journal of Solids and Structures 43 (7-8), 2318–2335.

Sakai, M., Sasaki, M., Matsuda, A., 2005. Indentation stress relaxation of sol-gel-derived organic/inorganic hybrid coating. Acta Materialia 53 (16), 4455–4462.

Stegall, D. E., Mamun, M. A., Crawford, B., Elmustafa, A. A., jan 2014. Repeated load relaxation testing of pure polycrystalline nickel at room temperature using nanoindentation. Applied Physics Letters 104 (4), 041902.

Stone, D. S., Jakes, J. E., Puthoff, J., Elmustafa, A. A., apr 2010. Analysis of indentation creep. Journal of Materials Research 25 (04), 611–621.

Syed Asif, S. a., Pethica, J. B., 1997. Nanoindentation creep of single-crystal tungsten and gallium arsenide. Philosophical Magazine A 76 (6), 1105–1118.

Varnik, F., Bocquet, L., Barrat, J.-L., feb 2004. A study of the static yield stress in a binary Lennard-Jones glass. The Journal of Chemical Physics 120 (6), 2788–2801.

Wehrs, J., Deckarm, M. J., Wheeler, J. M., Maeder, X., Birringer, R., Mischler, S., Michler, J., 2017. Elevated temperature, micro-compression transient plasticity tests on nanocrystalline Palladium-Gold: Probing activation parameters at the lower limit of crystallinity. Acta Materialia 129, 124–137.

Wehrs, J., Mohanty, G., Guillonneau, G., Taylor, A. A., Maeder, X., Frey, D., Philippe, L., Mischler, S., Wheeler, J. M., Michler, J., aug 2015. Comparison of In Situ Micromechanical Strain-Rate Sensitivity Measurement Techniques. JOM 67 (8), 1684–1693.

Xu, B., Yue, Z., Chen, X., 2010. Characterization of strain rate sensitivity and activation volume using the indentation relaxation test. Journal of Physics D: Applied Physics 43 (24).

Zhang, C. Y., Zhang, Y. W., Zeng, K. Y., Shen, L., Wang, Y. Y., 2006. Extracting the elastic and viscoelastic properties of a polymeric film using a sharp indentation relaxation test. Journal of Materials Research 21 (12), 2991–3000.